MNRAS **000**, 1–5 (2016) Preprint 6 October 2016 Compiled using MNRAS LATEX style file v3.0

Explaining unusual line profiles of SN 2006gy

Nikolai N. Chugai,[1⋆]
Institute of Astronomy Russian Academy of Science, Moscow, Russia

arXiv:1610.01352v1 [astro-ph.HE] 5 Oct 2016

Accepted XXX. Received YYY; in original form ZZZ

ABSTRACT

Origin of enigmatic line profiles of extremely luminous type IIn supernova SN 2006gy on day 96 is explored. Among conceivable possibilities the most preferred is the model that suggests holes in the optically thick cool dense shell (CDS). The line radiation emitted at the inner side of the opaque CDS escapes through the holes thus producing unusual line profile with the emission shifted redward. The holes could emerge as a result of the vigorous Rayleigh-Taylor instability leading to the CDS fragmentation. The model light curve with the CDS fragmentation is shown to be consistent with the SN 2006gy bolometric light curve.

Key words: supernovae – individual – SN 2006gy

1 INTRODUCTION

The supernova SN 2006gy is an exceptional case of strongly interacting type IIn supernovae (SNe IIn) because of the tremendous luminosity ($\sim 2\times10^{44}$ erg s^{-1}) and the radiated energy ($\sim 2\times10^{51}$ erg) (Smith et al. 2007; Ofek et al. 2007; Smith et al. 2008, 2010). To account for this phenomenon the ejecta with the energy $\gtrsim 3\times10^{51}$ erg must collide with a massive circumstellar (CS) envelope ($\sim 10\ M_\odot$), residing at the radius of $\sim 3\times10^{15}$ cm (Smith & McCray 2007). Unlike more common SNe IIn, the radiation generated by the shock wave in the SN 2006gy is strongly trapped for about two months due to a large optical depth (Smith & McCray 2007). Light curve modelling Moriya et al. (2013) based on the radiation hydrodynamics supports the picture of vigorous CS interaction and authors conclude that in this case SN ejecta of $\lesssim 15\ M_\odot$ and kinetic energy of $\gtrsim 4\times10^{51}$ erg collides with the $\approx 15\ M_\odot$ of CS matter (CSM). The origin of the tremendous mass loss by the pre-SN and the very explosion mechanism are not fully understood. A thermonuclear explosion initiated by the pulsating pair-instability of massive star ($\approx 100\ M_\odot$) so far is the only viable scenario (Woosley et al. 2007).

Despite a general consensus on the vigorous CS interaction as a cause for the SN 2006gy phenomenon, some crucial issues of the spectrum formation are not understood. The excellent spectral data and their comprehensive analysis (Smith et al. 2010) reveal narrow and broad lines on the continuum which at first glance look like what one expects in SN IIn. Yet Smith et al. (2010) come up with an interesting conclusion that broad line profiles, e.g., Hα and Fe II 5018 Å at the age $t \gtrsim 90$ d are highly unusual. While possible line-forming are discussed by Smith et al. (2010), the issue, what actually make the profiles odd, remains enigmatic.

I address the issue of the unusual broad lines in SN 2006gy in an attempt to find at least a qualitative explanation of the phenomenon. The line profile depends primarily on the kinematics of line-forming regions, geometry of continuum-emitting gas and its position relative to the line-forming regions. Different possibilities will be explored using Monte Carlo simulations and most probable interpretation will be proposed (section 2). I will check then, whether constraints from the sensible line profile model are consistent with the bolometric light curve (section 3). The results are summarized and discussed in the conclusion section.

2 SPECTRAL MODELING

2.1 Preview

SN 2006gy ejecta interact with a dense CSM in a strongly radiative regime which suggests that a cool dense shell (CDS) forms between the forward and reverse shocks (FS, RS). The CDS seems to be opaque for about 90 d and expands at $4000-5000$ km s^{-1} (Smith et al. 2010). The opaque geometrically thin and spherically symmetric CDS with the attached FS prevents the formation of pronounced broad absorption lines of low-ionization species. That is why we see in early SN 2006gy only smooth continuum originated from the CDS with the CS emission lines broadened by Thomson scattering (Smith et al. 2010) likewise, e.g., in SN 1998S (Chugai 2001). Between days 71 and 93 the SN 2006gy spectrum (cf. Smith et al. 2010) changes dramatically: relatively smooth continuum becomes bumpy and new emission lines suddenly emerge with growing luminosity, e.g., Ca II infrared

⋆ E-mail: nchugai@inasan.ru

© 2016 The Authors

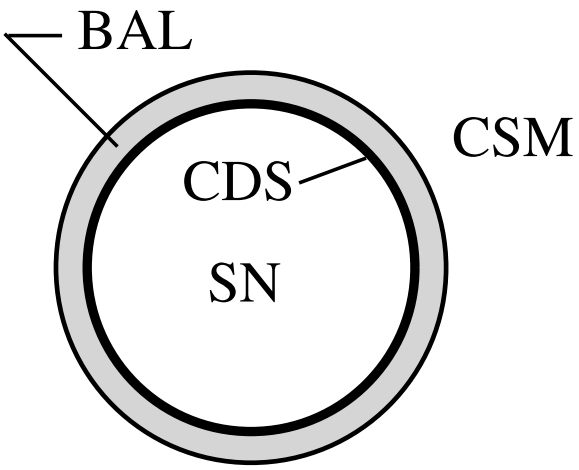

Figure 1. Sketch showing structure elements contributing to line profile formation in the model A. Unshocked ejecta (SN) are responsible for the bulk of a broad line emission; the partially transparent CDS produces continuum; the BAL layer is responsible for the broad line absorption and scattered emission; the unshocked CSM produces narrow lines.

triplet. This indicates that the opaque CDS becomes partially transparent at that epoch and line emission from the interior become visible. It is about this age that the Fe II 5018 Å and Hα lines acquire unusual profiles (Smith et al. 2010) (cf. also figure 2 below). The peculiar feature of these lines, most apparent in Fe II 5018 Å, is a red emission component flanked by a sharp blue cut-off at about zero radial velocity.

Smith et al. (2010) conjecture that peculiar line profiles are due to a blue absorption with the monotonically increasing depth towards zero radial velocity. The absorbing gas lies presumably between the FS and the CDS. This picture is called here the model A (or case A). Indeed, a cool absorbing gas can form a layer between the CDS and CSM due to the Rayleigh-Taylor instability (RTI) of the CDS and subsequent mixing of RT spikes in the FS (Chevalier 1982; Chevalier & Blondin 1995; Blondin & Ellison 2001). The major structure components involved in the broad line formation in the case A on day 96 then include the partially transparent CDS responsible for the continuum, the SN ejecta that produces broad emission lines partially attenuated by the CDS, and the outer broad absorption line (BAL) layer attached to the CDS (Fig. 1). The expected kinematics of the cool material in this case is the flow with almost constant velocity along the radius. The line profile in this case is well known and, anticipating simulations, unlikely able to fit the observed profiles. However, with some modification the model A still may be viable.

A partial transparency of the CDS in the considered epoch and especially a redshift of the broad emission lines by ≈ 1000 km s^{-1} which is apparent in Fe II 5018 Å and Ca II 8662 Å (cf. Smith et al. 2010) prompts an alternative possibility (model B). It suggests that a significant fraction of the line emission originates at the inner side of the opaque CDS and this emission escapes through the holes in the CDS possibly after the Thomson scattering and absorption in the unshocked ejecta. Note this model does not include BAL layer. The cartoon for the model B would be almost identical to Fig. 1 but the BAL layer.

Simulations of line profiles below are based on the Monte Carlo technique. Note that the models do not include narrow lines originated from the CSM.

2.2 Model A

The fiducial model A includes the partially transparent continuum-emitting CDS with the effective optical depth $\tau_s = 1$ and velocity $v_s = 5000$ km s^{-1}, the unshocked SN ejecta ($r < r_1 = 1$) with the terminal velocity $v_{sn} = 6000$ km s^{-1}, and the BAL layer ($r_1 < r < r_2 = 1.2$) with the constant velocity $v = v_s = 5000$ km s^{-1}. The line emissivity in the ejecta is adjusted to produce a sensible fit. The Sobolev optical depth is set to be constant in the line-absorbing layer which is not critical. The absence of the prominent emission component in the narrow component of Fe II 5018 Å line (cf. Smith et al. 2010) suggests that the scattering in this line is non-conservative, probably because of a photon destruction in a Rosseland cycle. This effect is taken into account assuming that the effective scattering albedo $\omega < 1$. The albedo stands for the ratio of the escaped radiation to the incident radiation and is defined through the Sobolev escape probability (β) and the photon destruction probability (ϵ) as $\omega = \beta/[\beta + (1-\beta)\epsilon]$. The shown model profile (Fig. 2a) is calculated for $\omega = 0.5$. In the case $\omega = 0.1$ the profile differs insignificantly and therefore is not plotted. The observed line profile, as expected, disfavours the fiducial model A with the constant velocity in the BAL layer.

The model A can be modified to produce more acceptable fit. To this end let us assume that the BAL layer contains an additional component related to the shocked CS clumps (if any) in the FS. The fragmentation and acceleration of shocked CS clumps can produce velocity spectrum of the cool gas in a broad range between the cloud shock and the forward shock speeds (Klein et al. 1994). We assume that the velocity distribution $f(v)$ of the cool gas in the BAL layer is uniform along the radius. The velocity presumably is dominated by the radial component $200 < v < 5000$ km s^{-1} with an additional isotropic random component $0 < u < 0.2v$. We show the case of $\omega = 0.1$ that is preferred compared to $\omega = 0.5$. The adopted velocity distribution is shown in the inset. The modified model A provides an overall description of the Fe II 5018 Å line (Fig. 2a) although the redshift of the emission is not reproduced. The same model, but $\omega = 1$, is applied to the Hα. The blue emission in this model is due to the resonant scattering in the BAL layer. The fit in the low velocity region is not good enough; parameter variations does not remove the disparity. In fact, a more serious problem with this model is that the SN 2006gy does not show an apparent signature of the CSM clumpiness. Indeed, the spectra do not show evidence for the intermediate component which usually is associated with shocked CS clumps.

2.3 Model B

The alternative case B includes three major components: an opaque CDS with transparent holes, unshocked SN ejecta, and a thin line-emitting layer at the inner side of the CDS.

Table 1. Parameters of illustrative models in case B.

Model	τ_t	τ_a	ω	f_{ej}
m1	1	1	0	0
m2	1	2	0	0
m3	2	2	0	0
m4	1	2	1	0
m5	1	2	0	0.4

The brightness of the outer and inner surface of the CDS in the continuum is assumed to be similar and isotropic. The intensity of the line radiation emitted by the inner side of the CDS is also assumed to be isotropic. The unshocked ejecta has large Sobolev optical depth and can be a source of the net line emission. The CDS velocity is $v_s = 5000$ km s^{-1} and the SN ejecta terminal velocity is adopted to be $v_{sn} = 7000$ km s^{-1}, the value consistent with the Fe II 4924 Å and 5018 Å lines and the light curve model, as we see below. The ejecta Thomson optical depth (τ_t), the absorption optical depths (τ_a), and hole covering factor (h) are free parameters.

The effect of parameter variations is shown in Fig. 3 with major parameters (Thomson optical depth, absorption optical depth, albedo, and fraction of net emission from the unshocked ejecta) given in Table 1. Results are not sensitive to the hole covering factor and $h = 0.3$ is adopted; this formally corresponds to the CDS effective optical depth of unity. The line profile is rather sensitive to the optical depth both τ_t and τ_a (Fig. 3a). The effect of the line scattering albedo is also strong (Fig. 3b) and thus can be easily constrained. The contribution of the line net emission from the SN ejecta with the fraction $f_{ej} = 0.4$ results in the significant modification of the line profile (Fig. 3c); this behaviour is crucial for the Fe II line and the Hα modelling.

The model B is applied first to both Fe II lines of 42 multiplet, 4924 Å and 5018 Å. These emissions in astrophysical objects have comparable fluxes with the 5018 Å line to be somewhat stronger. In the η Car spectrum (Zethson et al. 2012) the line intensity ratio $I(4924)/I(5018) = 0.68$; this value is used here. In SN 2006gy on day 96 the Fe II 4924 Å emission is significantly weaker and more narrow than 5018 Å. This is due to the absorption in the unshocked ejecta of 4924 Å redshifted photons by the 5018 Å line, the effect included in the model (Fig. 4). The red cut-off of the 4924 Å line emission is consistent with the adopted terminal velocity of the unshocked ejecta (7000 km s^{-1}), although noise does not permit to constrain this velocity better than ±1000 km s^{-1}. The Fe II net emission in the presented model fully originates from the inner side of the CDS. The line scattering albedo is constrained as $\omega < 0.2$; here $\omega = 0.1$ is used. Other parameters are $\tau_t = 0.7$, $\tau_a = 1.5$ (the uncertainty is 10-15%). The model describes the 4924 Å line not as good as the 5018 Å possibly because of an interference of the former with the Hβ emission; this effect is not included in the model. The Hα model, unlike the Fe II case, includes the net emission from unshocked ejecta with 24% of the total line emission rate. This permits us to describe the overall line shape, particularly. in the range of ±1500 km s^{-1}. Another difference is the larger absorption in the ejecta, $\tau_a = 2.2$ compared to 1.5 for Fe II lines. Generally this is expected since the absorption in the optical band increases from blue to red (Paschen continuum, H$^-$).

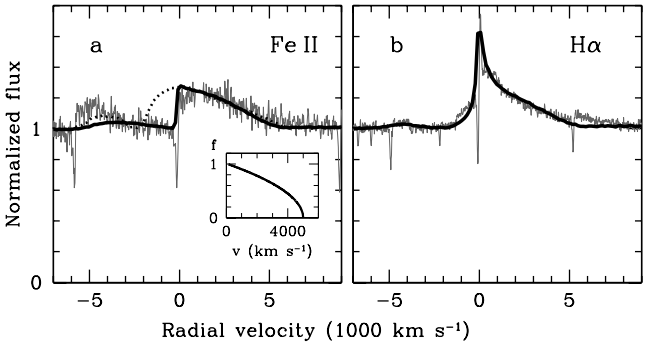

Figure 2. Fe II 5018 Å and Hα line profiles in SN 2006gy on day 96. Left panel: observed Fe II profile (grey thin line) compared to the model A with constant velocity in the BAL layer (dotted line); the model is strongly disfavoured by data. The modified model A with the random velocities of line-absorbing gas (thick line) fits data better. The inset shows the velocity distribution in the BAL layer. Right panel: observed Hα profile (grey thin line) with the overplotted model with the random velocity distribution in the BAL layer. The model is the same as for Fe II except for the larger line scattering albedo in the case of Hα.

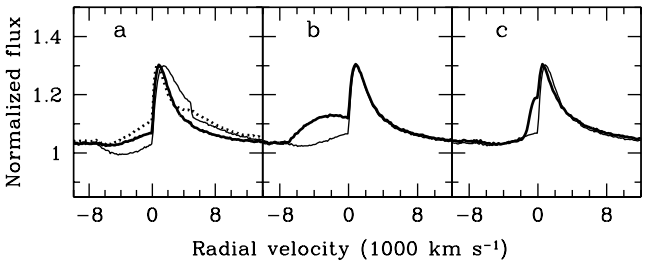

Figure 3. Illustrative models for case B (see Table 1). Left panel shows the model m1 (thin line), model m2 (thick line) with larger absorption, and model m3 (dotted line) with larger Thomson optical depth. Middle panel compares model m2 (thin line) and the model m4 with albedo $\omega = 1$. Right panel shows model m2 (thin line) and m5 that includes the line emission from ejecta.

Summing up, both Fe II 5018 Å line and Hα are described by the model B more successfully compared to the model A. Note, the model B easily reproduces the redshift of emission maximum of ≈ 1000 km s^{-1} in agreement with the observed redshift in Fe II 5018 Å and Ca II 8662 Å emissions (cf. Smith et al. 2010), whereas this effect is absent in the model A.

3 CDS FRAGMENTATION AND LIGHT CURVE

The proposed interpretation of the unusual line profiles in both models suggests that the CDS on day 96 is partially transparent, $\tau_s \sim 1$. This raises a question, whether the proposed CDS fragmentation is consistent with the bolometric light curve. To explore this issue the CS interaction model should be able to compute the bolometric light curve with the radiation trapping and the CDS fragmentation. This can be done in the framework of the model applied recently to the type IIn-P supernova SN 2011ht (Chugai 2016). Let us recap briefly the essential points of this model.

The model is based on a thin shell approximation

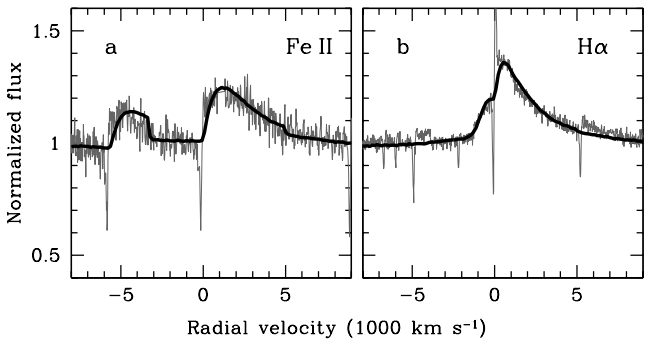

Figure 4. Fe II and Hα lines in SN 2006gy on day 96 (gray thin line) with the overplotted model B. Left panel shows Fe II 4924 Å and 5018 Å lines, and right panel shows Hα. The emission excess in the range of radial velocities 5000-7000 km s^{-1} is due to He I 6678 Å that is absent in the model.

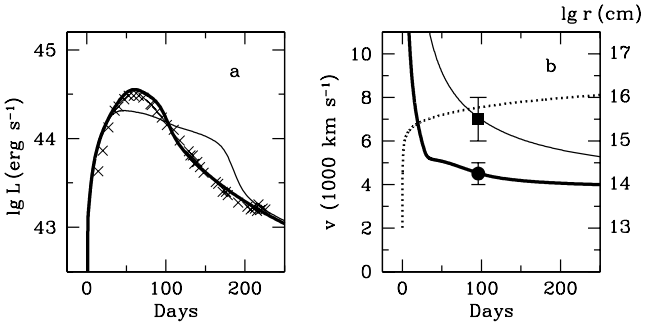

Figure 5. SN 2006gy light curve, velocity and radius. Left panel: the observed bolometric light curve (crosses) with overplotted models, viz. the model with fragmented CDS (thick line) and intact CDS (thin line). Right panel: the model CDS velocity (thick solid line), the terminal velocity of unshocked ejecta (thin solid line), and the CDS radius (dotted line). The points show the estimated velocity of the CDS (circle) and the terminal velocity of the unshocked SN ejecta (square) on day 96.

Giuliani (1982). The radiation trapping effects are described in a picture of a radiation bubble confined in an optically thick spherical shell. The bubble energy E_r is determined by the energy generation in shock waves, the work spent by the radiation on the shell expansion, and the radiation escape. The luminosity is defined as $L = E_r/t_d$ with the diffusion time $t_d = \xi(\tau+1)r_s/c$, where τ is the total optical depth, r_s is the shell radius, c is the speed of light, and ξ is a fudge factor adopted to be $\xi = 0.5$; this value corresponds to the diffusion time in the problem of a central point source in a homogeneous sphere (Sunyaev & Titarchuk 1980). The total optical depth of the ejecta, CDS and CSM is defined by the Rosseland opacity (Alexander 1975). The temperature distribution and the optical depth are recovered iteratively on the bases of the Eddington approximation, $T^4 = (3/4)T_{eff}^4(\tau+2/3)$ where T_{eff} is the effective temperature. Usually 4-5 iteration is enough to attain the accuracy of one percent. The thin shell density is set to be $\rho_s = 7\rho_{cs}$ (ρ_{cs} is a preshock CS density) in line with the density jump in the strong radiation-dominated shock. Unshocked supernova ejecta is assumed to expand homologously, ($v = r/t$) with the density $\rho \propto v^{-1}$ in inner layers and $\propto v^{-8}$ in outer layers. The density in the CS envelope expanding at the velocity 150 km s^{-1} is set by the broken power law $\rho \propto r^k$ with the density maximum at r_1, $k = k_1 > 1$ for $r < r_1$, $k = k_2 < 0$ for $r_1 < r < r_2$, and $k = k_3 < 0$ for $r > r_2$.

Keeping in mind that CDS is unstable with respect to RTI two cases are considered: intact and fragmented CDS. The CDS fragmentation is implemented via the effective optical depth of a clumpy medium

$$\tau = \tau_{oc}\left[1 - \exp\left(-\tau_0/\tau_{oc}\right)\right] , \quad (1)$$

(cf. Chugai 2016), where τ_0 is the optical depth of the intact CDS and τ_{oc} is the occultation optical depth, i.e., the average number of the CDS fragments (clumps) along the radius. The evolution of this value is set as

$$\tau_{oc} = \tau_{oc,0}\left[1 + \left(\frac{t}{t_f}\right)^4\right]^{-1} , \quad (2)$$

where for the optimal model $\tau_{oc,0} = 108$, and $t_f = 23$ d is the epoch of the fragmentation turn-on. Anticipating results, the right panel of Fig. 5 suggests the vigorous CDS deceleration favouring RTI takes place before day 30. The system of equations of motion, energy, and mass conservation is solved by the 4-th order Runge-Kutta. In each computed case the energy is conserved within 2%.

The overall properties of the light maximum are found to be an outcome of a collision between 9 $M_\odot$ SN ejecta with the kinetic energy of 5.3×10^{51} erg and CSM of 9 $M_\odot$, in general agreement with results of Moriya et al. (2013). Two cases are plotted: the intact and fragmented CDS (Figure 5). The CSM is set by the radii $r_1 = 3 \times 10^{15}$ cm, $r_2 = 6 \times 10^{15}$ cm, $r_3 = 2 \times 10^{16}$ cm, and power law indices $k_1 = 3$, $k_2 = -3$, and $k_3 = -5$. The model with the intact CDS poorly describes the observed bolometric light curve (Smith et al. 2010). Note that the "shoulder" at the age of 100-140 d is a specific feature not only to our model; a similar shoulder is present in the light curve models of SN 2006gy computed in the framework of the radiation hydrodynamics (Moriya et al. 2013, figure 5). In the model with the fragmentation the shoulder disappears and the overall fit gets better (Fig. 5). On day 96 the effective optical depth of the intact CDS is ≈ 15, whereas the optical depth of the fragmented CDS is ≈ 1.3, comparable to the CDS optical depth of the spectral model. Remarkably, the model CDS velocity on day 96 is 4500 km s^{-1}, close to the observational estimate $4000-5000$ km s^{-1} (Smith et al. 2010), and the model terminal ejecta velocity is also consistent with the estimate $v_{sn} \approx 7000$ km s^{-1} recovered from the Fe II line modelling.

To summarize, the CDS fragmentation invoked for the spectral model does not contradict to the bolometric light curve; moreover, the model with the fragmentation seems to be preferred.

4 CONCLUSIONS

The study has been aimed at the problem of the unusual line profile observed in the spectra of SN 2006gy after about day 90 (Smith et al. 2010). Two major conceivable models with the external BAL layer (model A) and without it (model B) have been explored and a more successful description of Fe II and Hα lines is found in the model B. It includes an opaque spherical CDS with transparent holes, a line-emitting layer at the inner side of the opaque CDS, and unshocked ejecta that can scatter the line radiation and be a source of a net

line emission as well. The success of rather simple model B indicates that essential physics is caught. Remarkably, the conjecture of the semi-transparent CDS at the age of 96 d turns out consistent with the bolometric light curve.

Yet the model B looks rather unconventional and poses some questions. The most critical point is the formation of the "punched" CDS. Although the Rayleigh-Taylor instability of the CDS is unavoidable, it is unclear whether the CDS fragmentation is able to produce a punched CDS with transparent holes. On the other hand, the fact that after about day 80 the luminosity of Hα and Ca II IR triplet rapidly increases, despite bolometric luminosity does not show a coeval change, suggests that the CDS actually becomes partially transparent at this age. Suppose, however, that holes are created, the next question then arises, whether the line emission rate is significantly larger at the inner side of the opaque CDS than at the outer side. To answer these questions direct numerical simulations are needed with the realistic high resolution 3D radiation hydrodynamics and 3D multi-group radiation transfer, which is currently beyond reach. For the time being, therefore, we are left with the situation when the unusual phenomenon is explained in the framework of a somewhat odd model. An encouraging aspect, however, is that the proposed explanation of the unusual line profiles in SN 2006gy can be considered as a starting point for the realistic look (beyond 1D) at the density and thermal structure of line-forming regions in SN 2006gy.

ACKNOWLEDGEMENTS

I thank Nathan Smith for kindly sending the spectrum of SN 2006gy. This work is supported by RNF grant 16-12-10519.

REFERENCES

Alexander D. R., 1975, ApJS, 29, 363
Blondin J. M., Ellison D. C., 2001, ApJ, 560, 244
Chevalier R. A., 1982, ApJ, 259, 302
Chevalier R., Blondin J. M., 1995, ApJ, 444, 312
Chugai N. N., 2001, MNRAS, 326, 1448
Chugai N. N., 2016, Astronomy Letters, 42, 82
Giuliani Jr. J. L., 1982, ApJ, 256, 624
Klein R. I., McKee C. F., Colella P., 1994, ApJ, 420, 213
Moriya T. J., Blinnikov S. I., Tominaga N., Yoshida N., Tanaka M., Maeda K., Nomoto K., 2013, MNRAS, 428, 1020
Ofek E. O., et al., 2007, ApJ, 659, L13
Smith N., McCray R., 2007, ApJ, 671, L17
Smith N., et al., 2007, ApJ, 666, 1116
Smith N., et al., 2008, ApJ, 686, 485
Smith N., Chornock R., Silverman J. M., Filippenko A. V., Foley R. J., 2010, ApJ, 709, 856
Sunyaev R. A., Titarchuk L. G., 1980, A&A, 86, 121
Woosley S. E., Blinnikov S., Heger A., 2007, Nature, 450, 390
Zethson T., Johansson S., Hartman H., Gull T. R., 2012, A&A, 540, A133

This paper has been typeset from a TEX/LATEX file prepared by the author.